A Predictive Direct Power Control Technique for Transformerless Grid Connected PV Systems Application

Nima Safari, *Student Member*, *IEEE*, Osama Aslam Ansari, *Student Member*, *IEEE*, and C.Y. Chung, *Fellow*, *IEEE*

***Abstract*— Transformerless grid-connected PVs are more economical and efficient compared to transformer connected PVs; however, in this type of connection high leakage current flows between the PV arrays and the grid due to the parasitic capacitances of the system. This leakage current is one of the main culprits in causing electromagnetic interference in power system, saturation of distribution transformers and poses safety issues. Common mode voltage (CMV) is primarily responsible for the existence of this leakage current. To cope with issues which arise from omitting galvanic isolation (transformer), in this paper a predictive direct power control (PDPC) with reduced common voltage (CMV) called active zero predictive direct power control (AZ-PDPC) is proposed. Both theory and simulation show that the proposed method reduces the level of CMV along with general good performance. The proposed method's characteristics are compared with the PDPC technique.**

***Index Terms*— Common mode voltage, leakage current, predictive direct power control model, reduced common mode voltage PWM, transformerless grid-connected PV**

I. Introduction

PHOTOVOLTAIC (PV) generation systems are becoming increasingly attractive and the number of grid-connected PV systems has significantly grown. Traditional grid-connected PVs utilize galvanic isolations either with high frequency DC-DC transformers on PV side or with low frequency transformers on grid side for reliability and safety aims. Both isolation methods ensure the elimination of leakage current and dc injection into the grid, but the latter type of isolation is bulky and costly, and the former is not efficient enough. For the aforementioned reasons, transformerless PV systems which are smaller, lighter, less expensive and highly efficient are recently developed [1]. As a result of omission of transformers, an excessive DC current known as leakage current results in problems such as safety issues and saturation of distribution transformers. For these reasons there are standards in place which require the limitation of the DC current component. As an example, according to VDE-0126-1-1 the leakage current must be restricted to a value lower than 300mA [2]. Leakage current mainly results from CMV variation which is generated in transformerless grid-connected inverters [3]. The leakage current resulted from CMV is called common mode current (CMC). Novel inverter topologies for suppressing the leakage current have been proposed [4]. However, most of them are presented for single phase systems.

Mainly, control of power converters can be realized by indirect power control or direct power control (DPC) approaches. In indirect power control approaches, pulse width modulation techniques are one of the essential building blocks. Modulation techniques that are based on prevention of applying zero voltage vectors which produce the highest amplitude of CMV have been proposed in PVs applications [3].

Due to complexity in tuning the parameters in indirect power control methods, DPC methods have been proposed. In [5], a modified DPC approach for minimizing the CMV amplitude to $\left|V_{dc}/6\right|$ is presented. In the CMV-minimized DPC, a switching table without zero vector is employed. However, the use of a fixed switching table can deteriorate the performance of power converter [6].

Along with increasing use of predictive control in diverse applications due to their efficiency and simplicity, several predictive current control and predictive DPC (PDPC) methods have been recently developed [6]-[8]. So far, in proposed PDPC methods, due to using zero vectors, the CMV amplitude can be as high as $\left|V_{dc}/2\right|$. This high level of CMV and the resultant CMC has made the application of PDPC limited. Considering this issue, in this paper an active zero PDPC (AZ-PCDPC) is presented. The proposed method shows a good performance in terms of reduction of CMV amplitude with minimum adverse impact on inverter performance.

The remainder of this paper is organized as follows. Section II presents CMV definition and the amplitude of CMV related to each switching state. CMV reduction in indirect power control strategies have been presented in Section III. In section IV, DPC and more specifically PDPC is illustrated. Using the CMV reduction methods in indirect power control, a direct power control method named AZ-PDPC is introduced in

The work was supported by the Natural Scientific and Engineering Research Council (NSERC), Canada. The authors are with the Department of Electrical and Computer Engineering, University of Saskatchewan, Saskatoon, SK S7N 5A9 Canada (e-mail: n.safari@usask.ca).

978-1-5090-1919-9/16/$31.00 ©2016 IEEE

Section V. Section VI evaluates the performance of the proposed method based on simulation in MATLAB/ SIMULINK. Section VII concludes this paper.

II. Common Mode Voltage

The CMV of a grid-connected inverter is defined as the voltage potential between star point and the midpoint of the DC voltage link (V_{no} in Fig. 1) [3]. In Fig. 1 the voltage of three phases on grid side are with respect to the ground and are denoted by V_{ga} , V_{gb} and V_{gc} . For three-leg inverter, by considering three-phase balance voltage for the grid, the CMV can be expressed as follows.

$$V_{n0} = \frac{V_{ao} + V_{bo} + V_{co}}{3} \tag{1}$$

where V_{ao} , V_{bo} and V_{co} represent the voltage on inverter side with respect to the middle point of the DC link.

The output voltage of a three-phase two-level inverter consists of eight different combinations of switching states which are shown in Table I. In this table the first six vectors are called active vector and the last two vectors are called zero vectors. Switching states and the CMV for each state are shown in Fig. 2. The leakage currents that flow through stray capacitances are proportional to the magnitude of CMV, variation of CMV and the stray capacitances of the system. Hence it is desirable to reduce the amplitude of CMV.

III. Indirect Power Control

The power controlling strategies developed for power converters can be mainly classified into direct control strategies and indirect control strategies. In indirect control approaches the reference signal is voltage and pulse width modulation (PWM) is used to compute the turn-on/turn-off times of the switches. Among indirect control approaches, space vector PWM (SVPWM) is widely used due to their superior performance [9]. In Fig. 2 the voltage vector with respect to each switching state is shown in α-β plane. In Fig. 2, θ is the angle between the reference voltage which is in *i*th sector and V_i. In classical SVPWM, at each sample time, the reference voltage is constructed by the combination of its nearest active vector and zero vectors [10]. Modulation index denoted by *M* indicates the utilization of inverter from DC link [11]. Modulation index can be calculated as follows:

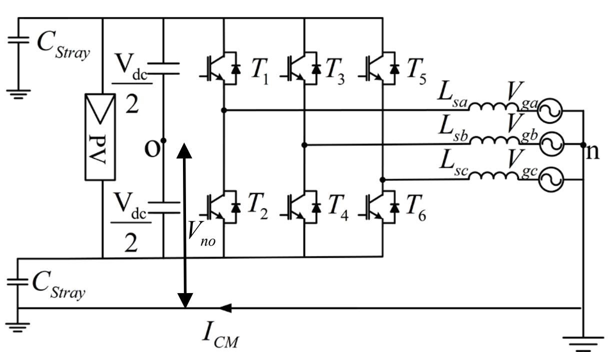

Fig. 1. The circuit diagram of a two level three-phase inverter.

TABLE I

SWITCHING STATES, OUTPUT VOLTAGES, AND CMV IN A THREE-LEG INVERTER

Vector	(T_1, T_3, T_5)	(V_{a0}, V_{c0}, V_{b0})	CMV
V_1	(1, 0, 0)	$(V_{dc}/2, -V_{dc}/2, -V_{dc}/2)$	$(-V_{dc}/6)$
V_2	(1, 1, 0)	$(V_{dc}/2, V_{dc}/2, -V_{dc}/2)$	$(V_{dc}/6)$
V_3	(0, 1, 0)	$(-V_{dc}/2, V_{dc}/2, -V_{dc}/2)$	$(-V_{dc}/6)$
V_4	(0, 1, 1)	$(-V_{dc}/2, V_{dc}/2, V_{dc}/2)$	$(V_{dc}/6)$
V_5	(0, 0, 1)	$(-V_{dc}/2, -V_{dc}/2, V_{dc}/2)$	$(-V_{dc}/6)$
V_6	(1, 0, 1)	$(V_{dc}/2, -V_{dc}/2, V_{dc}/2)$	$(V_{dc}/6)$
V_7	(1, 1, 1)	$(V_{dc}/2, V_{dc}/2, V_{dc}/2)$	$(V_{dc}/2)$
V_0	(0, 0, 0)	$(-V_{dc}/2, -V_{dc}/2, -V_{dc}/2)$	$(-V_{dc}/2)$

$$M = \frac{\pi}{2} \frac{V_{ref}}{V_{dc}} \tag{2}$$

SVPWM can be modified to reduce the CMV resulted from switching [3]. As it is obvious in Table I, zero vectors (V_7 and V_0) cause the highest CMV. In the switching method called active zero state PWM (AZSPWM), two active voltage vectors adjacent to reference voltage are used. Unlike conventional SVPWM, in AZSPWM instead of using zero vectors, two opposite active vectors with equal time are employed to effectively create a zero voltage vector. In AZSPWM, the maximum CMV is reduced to approximately 16% of DC link voltage ($V_{dc}/6$). There are several other CMV reduction approaches based on SVPWM and a comprehensive review of them can be found in [3]. However, among all of the existing SVPWM-based method, AZSPWM, is the only approach that can be used for a wide range of modulation index.

IV. Predictive Direct Power Control

Indirect power control techniques require many parameters to be tuned [4]. In this regard, various DPC frameworks have been developed [5], [12], [13]. Conventional DPC methods are generally based on a look up table and hysteresis band operators. It is obvious that the look up table cannot always provide the best switching decision in terms of tracking active power and reactive power. Moreover, conventional DPCs

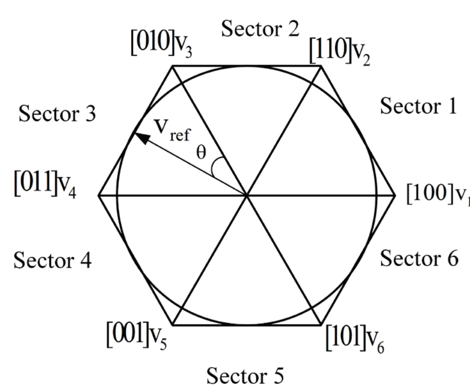

Fig. 2. Voltage vectors in α-β plane.

results in injecting considerable amount of harmonic components. For these reasons, PDPCs have recently been developed to address the problem related to conventional DPCs. In the following, a PDPC technique which is based on SVPWM is illustrated.

A three-phase voltage or current in *abc* frame of reference can be transformed into α-β domain as follows [14]:

$$\begin{bmatrix} U_\alpha \\ U_\beta \\ U_0 \end{bmatrix} = \frac{2}{3}\begin{bmatrix} 1 & -0.5 & -0.5 \\ 0 & \sqrt{3}/2 & -\sqrt{3}/2 \\ 1/2 & 1/2 & 1/2 \end{bmatrix}\begin{bmatrix} U_a \\ U_b \\ U_c \end{bmatrix} \tag{3}$$

where U can be current or voltage.

For a typical three-phase system the active power (P) and reactive power (Q) can be calculated as follows:

$$P(t) = \frac{3}{2}[V_{g\alpha}(t)i_\alpha(t) + V_{g\beta}(t)i_\beta(t)] \tag{4}$$

$$Q(t) = \frac{3}{2}[-V_{g\alpha}(t)i_\beta(t) + V_{g\beta}(t)i_\alpha(t)] \tag{5}$$

where $V_{g\alpha}$, $V_{g\beta}$, i_α and i_β are voltage and current components of the three-phase grid in α-β frame of reference, respectively.

For high sampling frequency it can be assumed that [13]:

$$\begin{aligned} V_{g\alpha}(k+1) &= V_{g\alpha}(k) \\ V_{g\beta}(k+1) &= V_{g\beta}(k) \end{aligned} \tag{6}$$

Considering this simplification, after discretizing (4) and (5), the difference equations (7) and (8) can be found, respectively.

$$\begin{aligned} P(k+1) - P(k) = \frac{3}{2}\Big[&V_{g\alpha}(k)\big(i_\alpha(k+1) - i_\alpha(k)\big) \\ &+V_{g\beta}(k)\big(i_\beta(k+1) - i_\beta(k)\big)\Big] \end{aligned} \tag{7}$$

$$\begin{aligned} Q(k+1) - Q(k) = \frac{3}{2}\Big[&V_{g\beta}(k)\big(i_\alpha(k+1) - i_\alpha(k)\big) \\ &-V_{g\alpha}(k)\big(i_\beta(k+1) - i_\beta(k)\big)\Big] \end{aligned} \tag{8}$$

On the other hand, using KVL and neglecting the effect of cable connecting inverter to the grid (Fig. 1), the mathematical model for a grid connected converter in α-β can be obtained.

$$\begin{cases} V_{I\alpha} - V_{g\alpha} = L\dfrac{di_\alpha}{dt} \\ V_{I\beta} - V_{g\beta} = L\dfrac{di_\beta}{dt} \end{cases} \tag{9}$$

where, $V_{I\alpha}$ and $V_{I\beta}$ are voltage components of three-phase inverter in α-β frame of reference, respectively. In (9), L represents the inductance of the filter connecting the inverter to the grid.

Applying the first order Taylor series approximation on (9) and considering (6), the variation of current components can be obtained as follows:

$$i_\alpha(k+1) - i_\alpha(k) = \frac{T_s}{L}\big(V_{I\alpha}(k) - V_{g\alpha}(k)\big) \tag{10}$$

$$i_\beta(k+1) - i_\beta(k) = \frac{T_s}{L}\big(V_{I\beta}(k) - V_{g\beta}(k)\big) \tag{11}$$

where T_s is the sampling period.

Substituting (10) and (11) in (7) and (8), the variation of active and reactive powers can be calculated as follows:

$$\begin{aligned} P(k+1) - P(k) = -\frac{3}{2}\frac{T_s}{L}\Big(&V_{g\alpha}^2(k) + V_{g\beta}^2(k) \\ &-V_{I\alpha}(k)V_{g\alpha}(k) - V_{I\beta}(k)V_{g\beta}(k)\Big) \end{aligned} \tag{12}$$

$$\begin{aligned} Q(k+1) - Q(k) = -\frac{3}{2}\frac{T_s}{L}\Big(&V_{I\beta}(k)V_{g\alpha}(k) \\ &-V_{I\alpha}(k)V_{g\beta}(k)\Big) \end{aligned} \tag{13}$$

In PDPC-based approaches the final objective is to ensure that active and reactive power become equal to their reference values at next sample time. Therefore, it can be concluded that:

$$P(k+1) = P_{ref}(k+1) \tag{14}$$

$$Q(k+1) = Q_{ref}(k+1) \tag{15}$$

Replacing (14) and (15) in (12) and (13) with considering (6), the required inverter voltage for next sampling step can be derived as follows:

$$\begin{aligned} V_{I\alpha}^*(k+1) &= V_{g\alpha}(k) + \frac{2}{3}\frac{L}{T_s}\frac{1}{\big(V_{g\alpha}^2(k) + V_{g\beta}^2(k)\big)} \\ &\Big[V_{g\alpha}(k)\big(P_{ref}(k+1) - P(k)\big) \\ &+V_{g\beta}(k)\big(Q_{ref}(k+1) - Q(k)\big)\Big] \end{aligned} \tag{16}$$

$$\begin{aligned} V_{I\beta}^*(k+1) &= V_{g\beta}(k) + \frac{2}{3}\frac{L}{T_s}\frac{1}{\big(V_{g\alpha}^2(k) + V_{g\beta}^2(k)\big)} \\ &\Big[V_{g\beta}(k)\big(P_{ref}(k+1) - P(k)\big) \\ &-V_{g\alpha}(k)\big(Q_{ref}(k+1) - Q(k)\big)\Big] \end{aligned} \tag{17}$$

After computing $V_{I\alpha}^*(k+1)$ and $V_{I\beta}^*(k+1)$, the reference vector for the next step can be obtained as follows:

$$V_{ref}(k+1) = V_{I\alpha}^*(k+1) + jV_{I\beta}^*(k+1) \tag{18}$$

Then the required switching states and the corresponding duration can be computed.

V. Active Zero Predictive Direct Power Control

PDPCs without considering CMV reduction methods, produce a high level of CMV and CMC. Therefore, they are not applicable for transformerless grid connected PVs. As it has been described in Section II, zero voltage vectors are mainly responsible for high CMV level. Therefore, in this paper the use of zero vectors in AZSPWM technique, is prevented and AZ-PDPC is developed. The simplified AZ-PDPC scheme is summarized in Fig. 3.

After computing the reference voltage for the next sample time using (18), if the reference vector lies in *i*th sector (Fig. 2), V_{ref} can be obtained by:

$$V_{ref}(k+1) = \frac{1}{2}\frac{t_0}{T_s}V_{i-1} + \frac{t_1}{T_s}V_i + \frac{t_2}{T_s}V_{i+1} + \frac{1}{2}\frac{t_0}{T_s}V_{i+2} \tag{19}$$

where t_0, t_1 and t_2 are the duration time in which zero vector and the two nearest active vector must be activated.

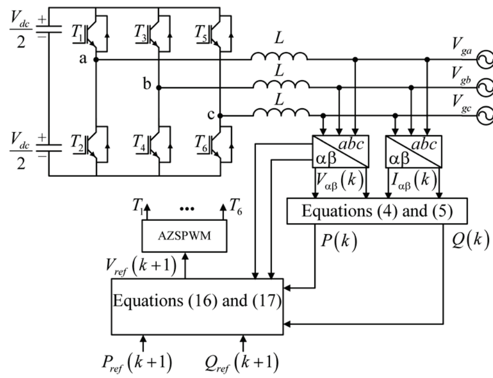

Fig. 3. Proposed AZ-PDPC control scheme.

As it is shown in (19), instead of using zero vectors two active vectors with opposite directions (V_{i-1} and V_{i+2}) have been employed. In (19), t_0, t_1, and t_2 can be easily found based on the projection of V_{ref} on its nearest active vectors as follows:

$$t_1 = \frac{2\sqrt{3}}{\pi} T_s \cdot M \cdot \sin(\frac{\pi}{3} - \theta) \tag{20}$$

$$t_2 = \frac{2\sqrt{3}}{\pi} \cdot T_s \cdot M \cdot \sin\theta \tag{21}$$

$$t_0 = T_s - t_1 - t_2 \tag{22}$$

VI. Simulation Results

In order to validate the performance of the AZ-PDPC and to compare it with PDPC, both methods are simulated on MATLAB/ SIMULINK. Simulation model for the proposed method is shown in Fig. 4. The main parameters of the system are given in Table II. The dynamic performance of PDPC and AZ-PDPC in controlling active power and reactive power are shown in Fig. 5 and Fig. 6 respectively. In these figure, at the beginning the values of active power and reactive power are set at 2 kW and 1 kVAR, respectively. Then, at t=0.15 s the reactive power is increased to 2 kVAR. Afterwards, at t=0.2 s, active power is increased to 3 kW.

CMV values for both AZ-PDPC and PDPC are plotted in Fig. 7 and Fig. 8, respectively. As it can be expected, the maximum amplitude of CMV in AZ-DPC is limited to $V_{dc}/6$. While maximum level of CMV in PDPC is $V_{dc}/2$. Hence there is a reduction of 66.67% in the maximum amplitude of CMV. This amount of CMV reduction can result in reduction in maximum CMV variation, thus the leakage current flowing through stray capacitance can be considerably remedied.

For further evaluation of dynamic behavior of AZ-PDPC, the three-phase current in AZ-PDPC method in the event of sudden increase from 3 kW to 5 kW in reference power is depicted in Fig. 9. As it is clear from figure, there are no transient issues in tracking step changes in reference power. The total harmonic distortion (THD) related to the inverter current for different active power values and for both AZ-PDPC and PDPC is plotted in Fig. 10. It can be seen that for values of active power more than 3.5 kW, the THD related to AZ-PDPC is very close to PDPC which agrees with the fact that for higher power generation, the modulation index increases, hence there will be less time for activation of zero vectors. Therefore, the PDPC will be similar to AZ-PDPC for wide range of output power of PV.

Therefore, based on above results, it can be concluded that the proposed method outperforms PDPC in solving the problem of CMV without adverse effect on THD compared against PDPC for a wide range of power.

TABLE II
System Parameters

Grid voltage	380 V
Grid frequency	50 Hz
DC link voltage	900 V
Inductance	100 mH
Switching frequency	10 kHz

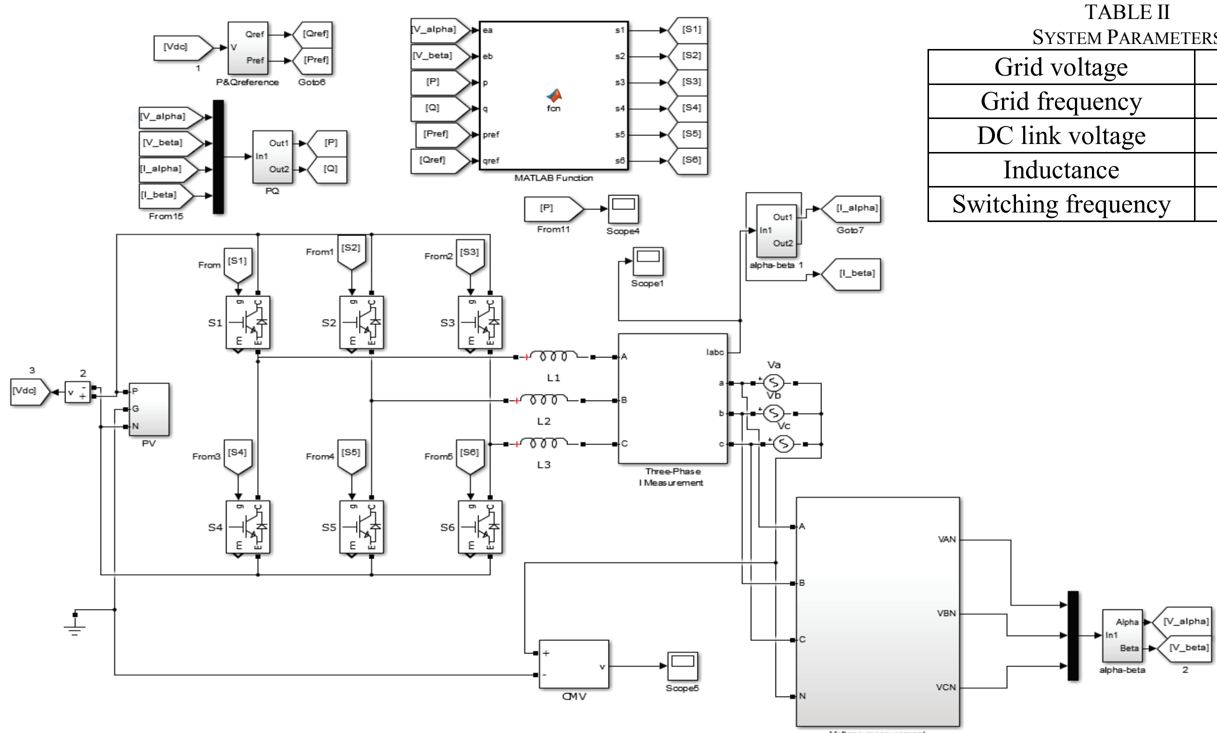

Fig. 4. Simulated system in MATLAB/ SIMULINK.

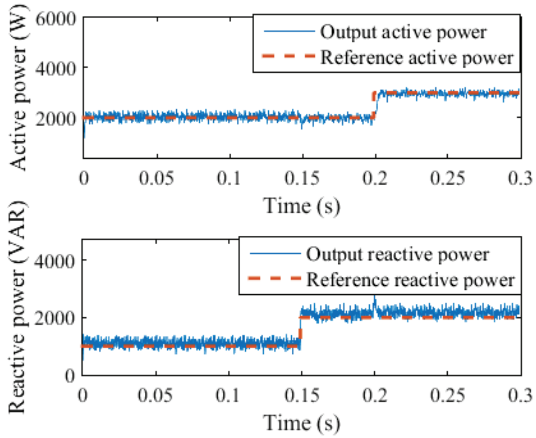

Fig. 5. Active power and reactive power control using AZ-PDPC.

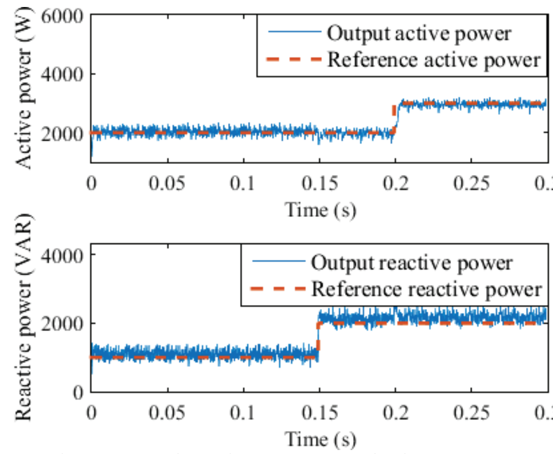

Fig. 6. Active power and reactive power control using PDPC.

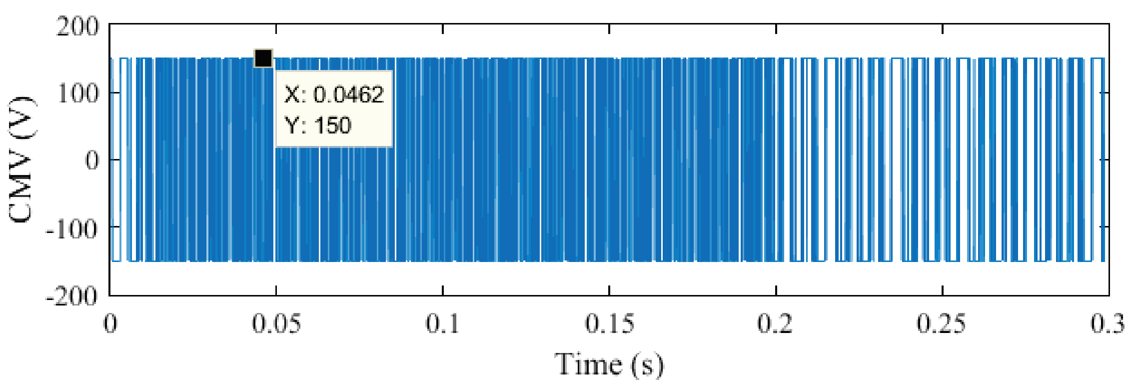

Fig. 7. CMV in AZ-PDPC.

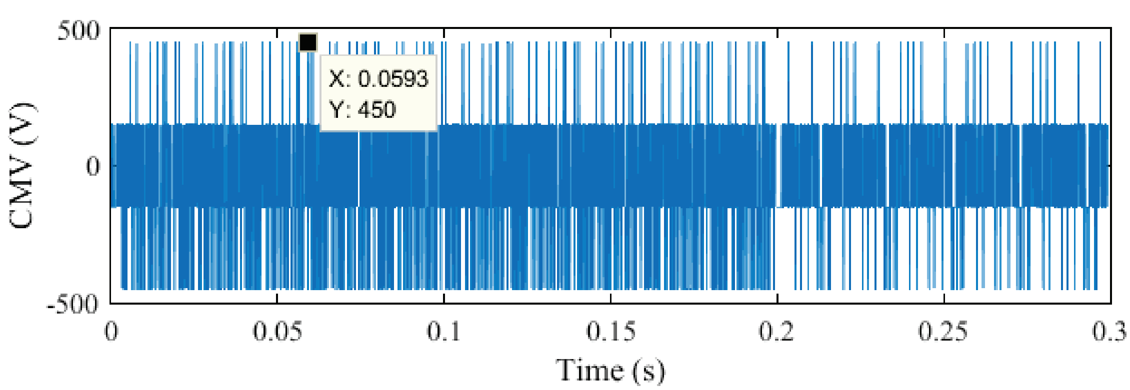

Fig. 8. CMV in PDPC.

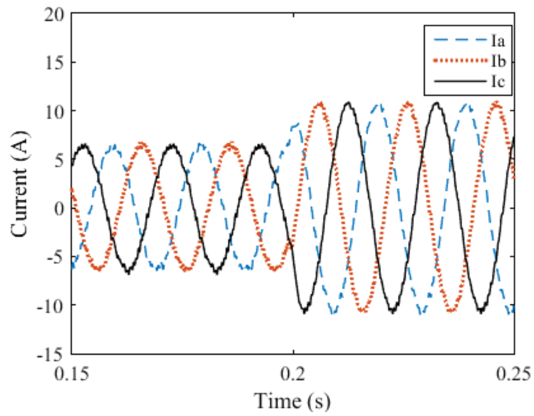

Fig. 9. Three-phase currents.

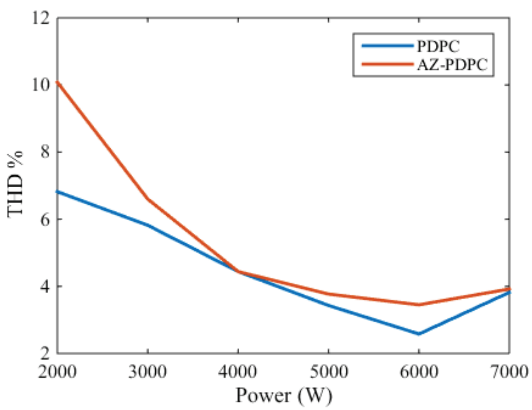

Fig. 10. Comparison of THD for different active power in PDPC and AZ-PDPC.

VII. Conclusion

Considering the low efficiency and high price of PV systems using galvanic isolation, transformerless PV systems are becoming more widely used. Therefore, the issues related to leakage current resulted from lack of galvanic isolation must be addressed in order to meet the requirements of different standards. This paper presents a power control strategy to lower the leakage current. Taking the advantages of predictive direct power control in this paper an active zero predictive direct power control is presented. As a result of the proposed control strategy the leakage current in the grid-connected transformerless PVs is reduced by a considerable amount. This method suppresses the amplitude of CMV to 16% of DC link voltage with an acceptable THD over a wide range of power.

References

[1] E. Koutroullis and F. Blaabjerg, "Design optimization of transformerless grid-connected PV inverters including reliability," *IEEE Trans. Power Electron.*, vol. 28, no. 1, pp. 325-335, Jan. 2013

[2] "Automatic disconnection device between a generator and the public low voltage grid," paragraph 4.7.1 photovoltaik, dke deutsche kommission elektrotechnik elektronik informationstechnik im din und vde, standard din vde 0126-1-1," Feb. 2006.

[3] C. C. Hou, C. C. Shih, P. T. Cheng, and A. M. Hava, "Common-mode voltage reduction pulsewidth modulation techniques for three-phase grid-connected converters," *IEEE Trans. Power Electron.,* vol. 28, no. 4, pp. 1971-1979, Apr. 2013.

[4] W. H. Li, Y. J. Gu, H. Z. Luo, W. F. Cui, X. N. He, and C. L. Xia, "Topology review and derivation methodology of single-phase transformerless photovoltaic inverters for leakage current suppression," *IEEE Trans. Ind. Electron.,* vol. 62, no. 7, pp. 4537-4551, Jul. 2015.

[5] B. Rueckert and W. Hofmann, "Common mode voltage minimized direct power control of the grid side connected converter in doubly fed induction generators," in *Proc. IEEE-SDEMPED,* Ischia, Italy, Jun. 11-12, 2008, pp. 1455-1459

[6] X. Wang and D. Sun, "Three-vector based Low-complexity Model Predictive Direct Power Control Strategy for Doubly Fed Induction Generator," *IEEE Trans. Power Electron.,* vol. PP, no. 99, pp. 1-1, Feb 2016.

[7] N. Safari, A. Khoshooei, and J. Moghani, "A new model predictive current controller with common mode voltage alleviation in three-phase inverters," in *Proc. 4th International eConf. on Computer and Knowledge Engineering,* Mashhad, Iran, 2014, pp. 474-478.

[8] Z. F. Song, W. Chen, and C. L. Xia, "Predictive direct power control for three-phase grid-connected converters without sector information and voltage vector selection," *IEEE Trans. Power Electron.,* vol. 29, no. 10, pp. 5518-5531, Oct. 2014.

[9] W. Ahmed and S. M. U. Ali, "Comparative study of SVPWM (space vector pulse width modulation) & SPWM (sinusoidal pulse width modulation) based three phase voltage source inverters for variable speed drive," in *Proc. IOP Conference Series: Materials Science and Engineering*, 2013, p. 012027.

[10] V. H. Prasad, "Analysis and comparison of space vector modulation schemes for three-leg and four-leg voltage source inverters," in *Proc. 12th Annual Applied Power Electronics Conf. and Expo.,* Atlanta, 1997, pp. 864-871.

[11] E. Ün and A. M. Hava, "A near-state PWM method with reduced switching losses and reduced common-mode voltage for three-phase voltage source inverters," *IEEE Trans. Ind. Appl.,* vol. 45, no. 2, pp. 782-793, Mar 2009.

[12] S. Aurtenechea, M. A. Rodriguez, E. Oyarbide, J. R. Torrealday, "Predictive Direct Power Control - A New Control Strategy for DC/AC Converters," in *Proc. 32nd Annual Conf. on IEEE Industrial Electronics*, Paris, IECON 2006, pp. 1661-1666.

[13] A. Bouafia, J.-P. Gaubert, F. Krim, "Predictive direct power control of three-phase pulsewidth modulation (PWM) rectifier using space-vector modulation (SVM)," *IEEE Trans. Power Electron.,* vol. 25, no. 1, pp. 228-236, Jan 2010.

[14] P. Krause, O. Wasynczuk, S. D. Sudhoff, S. Pekarek, *Analysis of electric machinery and drive systems,* USA: Wiley-IEEE, 2013.